Study on Microstructure and Mechanical Properties of Al-Mg-Si-Cu Aluminium Alloy with High Ductility

Guanxia Xue [1], *Gu* Zhong [1,*], *Shipeng* Lin [1], *Hu-Tian* Li [2], *Xinghui* Gui [1], and *Lei* Zhang [3,4]

[1]Chinalco Materials Application Research Institute Co., Ltd., Suzhou Branch, Suzhou 215026, China
[2]Chinalco Materials Application Research Institute Co., Ltd., Beijing 102209, China
[3]Biomanufacturing Center, Department of Mechanical Engineering, Tsinghua University, Beijing 100084, China
[4]Biomanufacturing and Rapid Forming Technology Key Laboratory of Beijing, Beijing 100084, China

Abstract. A new type of Al-Mg-Si-Cu aluminium alloy with high ductility was studied in the present work. The microstructure features and mechanical properties of this alloy were systematically characterized by scanning electron microscopy (SEM), electron back-scatter Diffraction (EBSD), high resolution transmission electron microscopy (HRTEM) and tensile and fatigue test. The percentage of sub-grain boundary under forging and aging process reaches up to 72% which can be attributed to the suppression of recrystallization by the nano-sized AlMnCrSi dispersoids. The combination of mechanical properties of the new alloy product in aged state showed that the ductility keeps in the range of 15~18%, yield strength and tensile strength are 310MPa and 380MPa respectively, fatigue strength ranges from 130MPa to 135MPa. It presents more excellent properties than commercial 6061 alloy for the nano-sized AlMnCrSi dispersoids, initial-β" precipitates and high percentage of sub-grain boundary.

Keywords: Microstructure; Mechanical Property; Al-Mg-Si-Cu Aluminum alloy; High Ductility

1. Introduction

6xxx series aluminum alloys are extensively used as structural parts of vehicles due to their excellent combination of properties, such as medium strength, formability, good corrosion resistance, weldability, and low manufacture cost [1-3]. Traditional forged vehicle parts are made of commercial 6061 alloy, which possess yield strength, tensile strength and ductility up to 280MPa, 320MPa, 10%-12% respectively. In consideration of energy conservation and environmental protection, lightweight is the development trends in automotive industry. Nowadays, in order to reduce weight of the vehicle forging parts, studies focus on developing high strength aluminum alloy through alloying compositions optimization, heat treatment and processing technology [4-8]. The microstructure and mechanical properties of Al–Mg–Si–Cu alloy with high manganese content are studied. The dominant strengthening precipitates comprising the needle-shaped pre-β″or β″ ($(Al+Mg)_5Si_6$ or Mg_5Si_6) and lath-shaped Q′ ($Al_3Cu_2Mg_9Si_7$) phases are identified in the T6 temper. With the increase of magnesium content, S (Al_2CuMg) phase is promoted to precipitate to give an enhancement in strength. The yield strength of the examined alloys with high manganese content is up to 380MPa, which is 50% higher than that of commercial 6061 alloy. It is considered that, in addition to the strengthening precipitates, Mn dispersoids generating the dispersion hardening effect and the homogeneous deformation contribute a lot to the favorable mechanical properties [9.10].

Traditional forging process of vehicle parts is relatively complicated, usually more than two-step. For example, forged hubs of 22 inches commercial vehicle of commercial 6061 alloy are produced by two-step forge and one-step spinning process [11]. However, in order to further save cost, improve fatigue resistance, and lightweight auto parts of 6xxx series aluminum alloy by using one-step forging process, developing high toughness Al–Mg–Si–Cu alloy is necessary.

In this paper, a new type of Al-Mg-Si-Cu aluminum alloys with high ductility was studied. The microstructure features and mechanical properties of this aluminum alloy were systematically determined by SEM, HRTEM and tensile test respectively.

2. Experimental procedure

2.1 Material preparation

The chemical composition of the new Al–Mg–Si–Cu alloy studied is listed in Table 1. The content of excess Si was controlled from 0.1 to 0.5. The material was prepared as follows.

* Corresponding author: zghust@qq.com

Table 1. The chemical composition of the Al–Mg–Si–Cu alloy used in the present work (wt.%).

Element	Si	Fe	Mg	Mn	Cu	Ti	Cr	Al
Content	0.746	0.141	0.73	0.653	0.427	0.024	0.268	Bal

(i) The billets of this new alloys were prepared experimentally by direct-chill (DC) casting, which was of 154 mm in diameter and 2500 mm in length. All billets were machined to make samples with 130 mm in diameter and 300 mm in length.

(ii) In order to eliminate elemental micro-segregation and form Mn and Cr containing dispersoids homogeneously, the homogenization treatment at 560℃ for 5h subsequently air-cooled was carried out for these samples.

(iii) After homogenization treatment, samples were hot forged at 450℃~500℃ to make 120 mm thick plates with the reduction ratio of 60%.

(iv) The forged plates were solution treated at 560℃ for 3 h and quenched into water at room temperature. The subsequent aging for a short-time was performed at 160℃~170℃ for 2h~3h in an air furnace.

2.2 Characterization

Microstructural observation of the studied Al–Mg–Si–Cu alloy was performed by using a 15 kV JSM-6480 type scanning electron microscope (SEM) and the type of intermetallic phases was identified by energy dispersive system (EDS). The effect of homogenization treatment on the percentage of sub-grain boundary was determined by examining hot forged specimens using electron back-scatter diffraction (EBSD) technique. The surface of the examined specimens was mechanical polished and electrochemical polishing sequentially. The experimental data were collected using a JSM-6480 type scanning electron microscope operating at 25kV with a TSL orientation imaging system. OIM analysis 4.6 software was used to analyze the EBSD map. The scanned area was typically 100um×240um with a step size of 0.8um. At least three different areas were selected and the reported results were the average values. The morphology and distribution of nano-precipitates of AlMnCrSi dispersoids during the homogenization annealing and forged process and aging treatment were investigated using transmission electron microscopy (TEM), JEOL-2100F. The morphology and distribution of aged precipitates were investigated by using high resolution transmission electron microscopy (HRTEM) with the symmetric condition along Al (001) axes. Thin foils for TEM study were prepared by first mechanical polishing to a thin foil about 80 um and then electro-polishing in a methanol solution mixed with 30% nitric acid and 70% alcohol. To evaluate the strength and ductility of the examined alloys, tensile tests were carried out. The tensile tests were conducted on an Instron 5967 30KN Materials testing machine operated at a constant crosshead speed with an initial strain rate of 5×10^{-4} s^{-1}. The tensile specimens were machined perpendicular to the forging direction as GB/T228.1-2010 standard with the gauge length of 50 mm. The schematic of tensile specimen is depicted in Fig. 1(a). As for tensile test, three specimens were tested and the average value was taken. High cycle fatigue (HCF) tests were obtained for constant amplitude loading with sinusoidal wave forms. The fatigue life tests (S-N curves) were carried out on specimens (midsection diameter 5.0 mm). These tests were performed at R = - 1 using MTS Landmark 370.10 fatigue testing machine with a frequency of 60 Hz. The S-N curves were measured in laboratory air. The schematic of fatigue specimen is depicted in Fig. 1(b). The final surface finish of the fatigue specimen after machining requires 0.32 and no further operation is carried out.

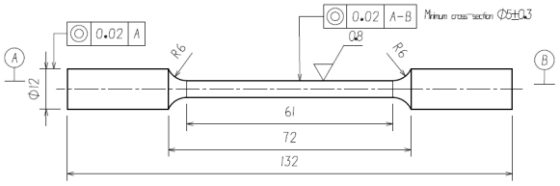

(a)

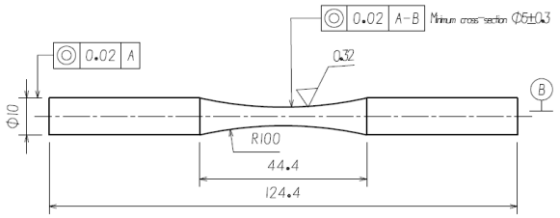

(b)

Fig.1. Schematics of the test specimens
(a) tensile specimen; (b) fatigue specimen.

3 Results and discussion

3.1 Microstructural characterization

The as cast microstructures of the new Al–Mg–Si–Cu alloy is shown in Fig.2. Substantial distinct intermetallic constituents are observed in the α-Al inter-dendritic regions, forming almost continuous network. Fig. 3 shows higher magnification microstructure of the different intermetallic constituents, which contain three intermetallic phases: Mg_2Si, Al(Fe,Mn,Cr)Si and AlCuMgSi. They were identified by a combination of morphology and EDS analysis (Table 2). The Al(Fe,Mn,Cr)Si intermetallic compound, which commonly known as α-phase, with a typical feathery structure or lamellar morphology, is the dominant phase in this new Al–Mg–Si–Cu alloy. Mg_2Si phase appears as needle-shaped or Chinese script-like structure. A small

* Corresponding author: zghust@qq.com

quantity of AlCuMgSi phases with round or oval-shaped morphology were observed to form as separate phase in the inter-dendritic regions.

In as cast Al–Mg–Si–Cu alloys, the remaining content of Si which does not form intermetallic compound Mg_2Si is defined as excess Si. Generally, the more excess Si the alloy contains, the higher tensile strength and yield strength will be [9]. In our opinion, a small amount of excess Si, ranging from 0.1 to 0.5 wt.%, is favorable for improving the ductility of the Al–Mg–Si–Cu alloy while ensuring the tensile strength and yield strength of the alloy. It can be found that, in Fig.3, in as cast microstructure of the Al–Mg–Si–Cu alloy, two intermetallic phases with excess Si are Al (Fe,Mn,Cr)Si and AlCuMgSi. In Table. 2, based on the EDS analysis, the average composition of the Al (Fe,Mn,Cr)Si phase are 72.33wt.% Al, 20.78 wt.% (Mn+Cr+Fe), and 6.89 wt.% Si. It is close to α-$Al_{15}(Fe,Mn)_3$-Si_2 as reported in literature[11]. The AlCuMgSi phase has a variable copper content from 5.64 to 10.01 mass% depending on Mg/Si ratio.

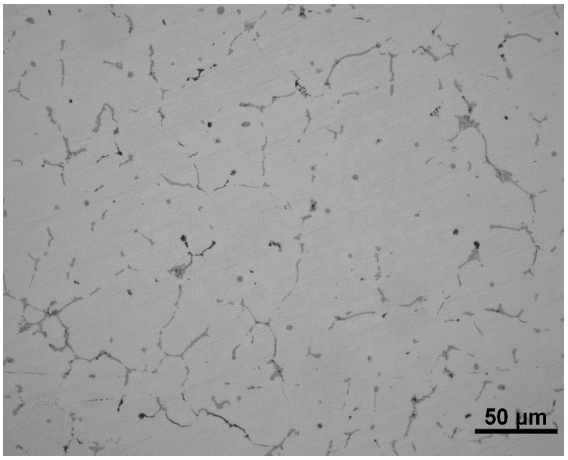

Fig.2. Microstructure of the new Al–Mg–Si–Cu alloy in as-cast state

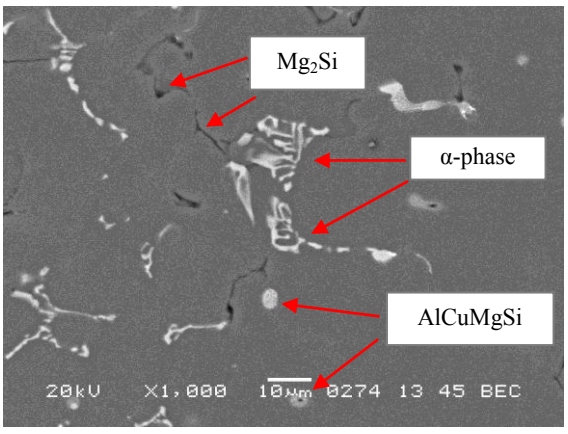

Fig.3. Higher magnification microstructure of the new Al–Mg–Si–Cu alloy showing the different morphology of intermetallic constituents.

Table 2. Composition of the experimentally observed intermetallic phases in Fig. 3 (wt.%).

Phase	Mg	Si	Cu	Cr	Mn	Fe	Al
Mg_2Si	8.44	11.77	-	-	-	-	79.79
	8.99	12.74	0.49	-	-	-	77.78
α-phase	1.00	7.01	1.21	2.22	8.00	9.20	71.37
	0.96	3.40	0.99	1.10	5.76	6.57	81.22
AlCuMgSi	4.17	10.57	8.14	-	-	-	77.12
	2.00	8.80	10.01	-	-	-	79.19

The microstructure of this new alloy after homogenization annealing is shown in Fig. 4. The majority of Mg_2Si and the all of AlCuMgSi phases were dissolved into the Al matrix. It can be seen from Fig. 5 that there was a fragmentation and spheroidization of the α-phase with distribution along boundaries after homogenization annealing.

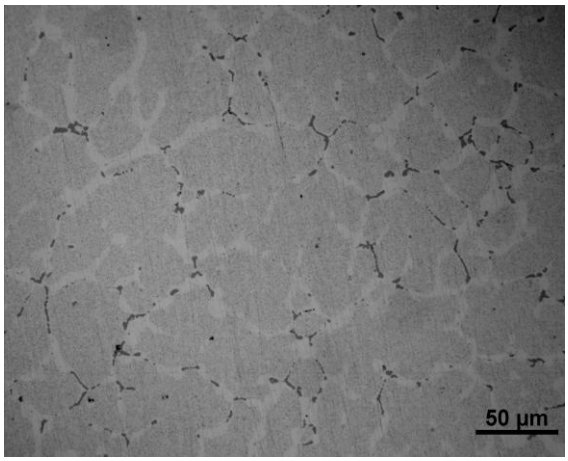

Fig.4. Microstructure of the new Al–Mg–Si–Cu alloys after homogenization annealing at 560℃ for 5h.

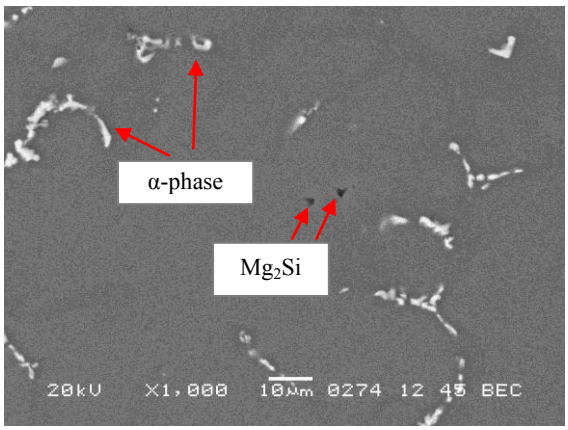

Fig.5. Higher magnification microstructure of the new Al–Mg–Si–Cu alloy after homogenization annealing at 560 ℃ for 5h showing an obvious fragments of α-Al(Fe,Mn,Cr)Si phase.

The EBSD micrograph of the new Al–Mg–Si–Cu alloys after hot forging with homogenization heating rate 7℃/min is shown in Fig.6. The different color contrast in the EBSD maps is corresponding to different grain orientation. The severely fragmented and elongated sub-grains like thin ribbon are observed. Through statistical analysis, the percentage of sub-grain boundary of the

new Al–Mg–Si–Cu is 72%, which is 20% higher than that of 6061 alloy. The higher percentage of sub-grain boundary, the higher ductility of the new Al–Mg–Si–Cu alloy will be. It is responsible for the highly uniform precipitation and dispersion characteristics of dispersoids during homogenization annealing in the new Al–Mg–Si–Cu alloy with appropriate amount of excess Si (in the range of 0.1-0.5wt.%), which play a critical role in preventing the nucleation of recrystallized grains during forging process and solution treatment [12]. The uniform precipitation dispersoids during homogenization annealing in the new Al–Mg–Si–Cu alloy with appropriate amount of excess Si will be illustrated with HRTEM observation in detail.

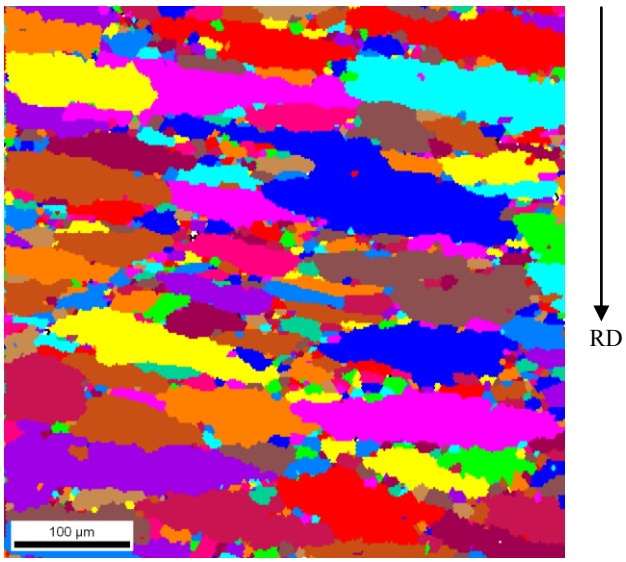

Fig.6. EBSD micrographs of the new Al–Mg–Si–Cu alloy after hot forging process.

3.2 HRTEM observations in material preparation

Fig. 7a shows a TEM bright-field images obtained from this new Al–Mg–Si–Cu alloy homogenized at 560℃ for 5 h and subsequently air-cooled. It can be found that numerous rod-like or cube-like nano-precipitates of AlMnCrSi dispersoids in size of 100-500nm, distribute dispersedly in Al matrix. Fig. 7b shows a TEM bright-field images obtained from this new Al–Mg–Si–Cu alloy after forging process. During the forging process, the grains are broken into small ones relatively. Simultaneously, the size and distribution of the nano-sized AlMnCrSi dispersoids also change. It can be seen, that most of the AlMnCrSi dispersoids locate in grain boundary and its size reduce to 50-200nm. The effect of nano-sized AlMnCrSi dispersoids on pinning grain boundary is better for preventing the nucleation of recrystallized grains during forging process and make grains smaller. Therefore, the percentage of sub-grain of the new Al–Mg–Si–Cu alloys after forging process is higher than the percentage of sub-grain of 6061 alloy. Fig. 7c shows a TEM bright-field images obtained from this new Al–Mg–Si–Cu alloy after aging treatment. During the aging treatment, the size and shape of the remained nano-sized AlMnCrSi dispersoids also change simultaneously. It can be seen, that the shape of the AlMnCrSi dispersoids has become rounded and its size reduce to 20-100nm furtherly.

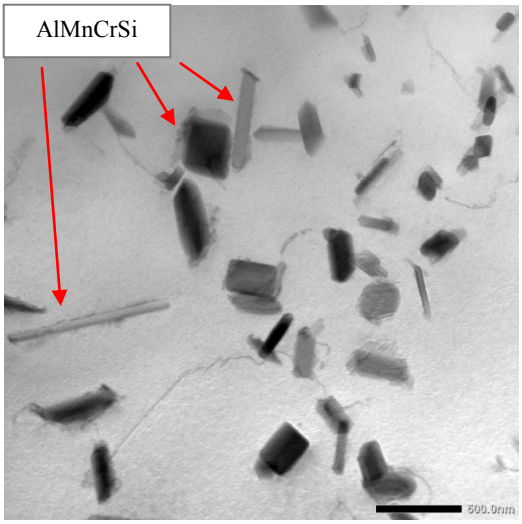

(a)

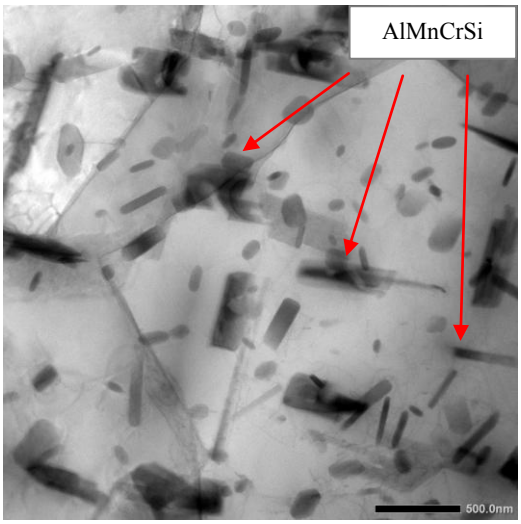

(b)

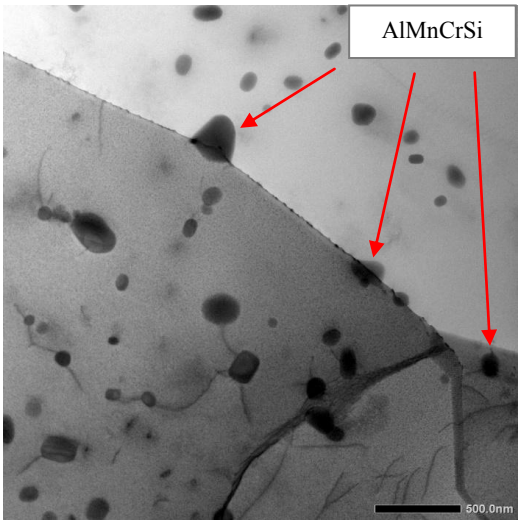

(c)

Fig. 7. TEM micrographs of AlMnCrSi dispersoids in the new Al–Mg–Si–Cu alloy: (a) dispersion distribution after homogenization annealing; (b) uniform distribution in the matrix after forge process; (c) uniform distribution in the matrix after aging treatment.

Commonly, the precipitation sequence in the matrix of 6xxx series alloys after aging treatment is as follows: Supersaturated solid solution – clusters – GP zones and initial-β" – pre-β", β" and Q" – Q' (partially coherent version of Q) and β (or β') – Q and β. Meanwhile, for Al–Mg–Si–Cu alloys, two types of strengthening phases, needle-shaped pre-β" and lath-shaped Q' precipitates, would precipitate in the T6 temper at 170-180℃ [10,11,15,16]. However, the precipitated phase of this new Al–Mg–Si–Cu alloy taken an aging of low-temperature and shot-time treatment is different compared to T6 temper of 6061 alloy.

Fig. 8(a) shows a TEM bright-field images obtained from this new Al–Mg–Si–Cu alloy aged at 160℃~170℃ for 2h~3h. A great number of aged nano-precipitates, AlMnCrSi dispersoids, are delineated by strain-field contrast. HRTEM micrographs further reveals only one type of strengthening phase, needle-shaped initial-β" precipitates, whose composition is $Mg_2Si_3Al_6$ (Fig. 8b). The initial-β" precipitate is generally considered as the precursor of pre-β" ($(Al+Mg)_5Si_6$) or β" (Mg_5Si_6) [10,14-16]. The needle-shaped initial-β" precipitate is oriented along the Al <001> direction. As shown in Fig. 8b, the cross section of aged nano-precipitates is observed making its diameter measurable accurately. The average diameter of initial-β" precipitate is about 2–3 nm. In addition, the needle-shaped initial-β" precipitate oriented along the Al <001> direction is also observed lying in Fig. 8b, which is nearly 8-10nm length.

Furthermore, the remained nano-sized AlMnCrSi dispersoids after the aging treatment distributed dispersedly and uniformly in the grain and on the grain boundary. When the fatigue crack propagates, these AlMnCrSi dispersoids can prevent crack growth further. So, the fatigue life of the new Al–Mg–Si–Cu alloy products may be improved.

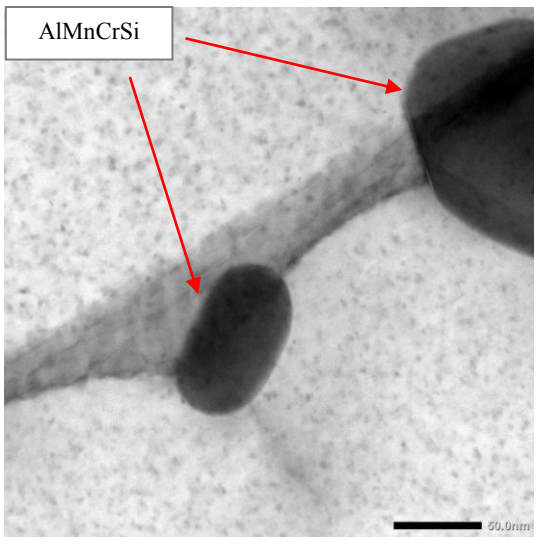

(a)

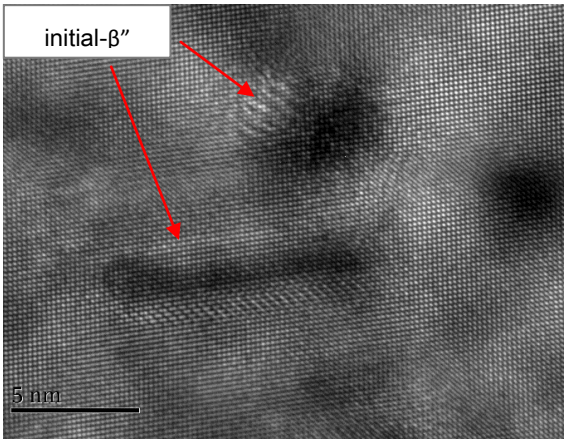

(b)

Fig. 8. TEM images of the new Al–Mg–Si–Cu alloy: (a) bright-field micrograph along with [001]Al; (b) HRTEM micrographs of needle-shaped initial-β" precipitates imaged along their axes.

3.3 Mechanical properties

The combination of mechanical properties of the new Al–Mg–Si–Cu alloy in aged state are given in Table 3. Compared with the commercial 6061 alloy, both strength and ductility of this new alloy increase significantly. Table 3 shows that the elongation is stable in the range from 15% to18%, yield strength and tensile strength are 310MPa and 380Mpa, respectively. In summary, the ductility and strength of this new Al-Mg-Si-Cu aluminum alloy are 35 percent and 11 percent higher than the commercial 6061 alloy.

The excellent ductility of this new alloy can be attributed to the uniform precipitation and dispersion characteristics of nano-sized AlMnCrSi dispersoids during homogenization annealing process and then the nano-sized AlMnCrSi dispersoids pinned the grain boundary to improve the ratio of sub-grain during the forging and heat treatment process, subsequently. As a result, the ratio of sub-grain boundary in the annealing microstructure, forging microstructure and age-state microstructure can be improved. So, the ductility of the Al–Mg–Si–Cu alloy is improved while ensuring its tensile strength and yield strength. Furthermore, the needle-shaped phase of the initial-β" precipitates during the aging treatment can further improve the ductility. Moreover, nano-sized AlMnCrSi dispersoids also can improve the fatigue life of the new Al–Mg–Si–Cu alloy products as mentioned above in section 3.2.

Table 3. Mechanical properties of the new Al-Mg-Si-Cu alloys and commercial 6061 alloy

Alloy		Ultimate tensile strength (MPa)	Yield strength (MPa)	Elongation (%)	Fatigue strength (MPa)
New alloy	Test 1	391	320	16.0	135
	Test 2	387	310	16.3	134

	Test 3	385	312	18.0	132
6061 alloy		290	255	13.0	118

4. Conclusion

1. The as cast microstructures of the new Al–Mg–Si–Cu alloy contain three intermetallic phases: Mg_2Si, Al(Fe,Mn,Cr)Si and AlCuMgSi, Which present in nano-sized rounded AlMnCrSi dispersoids about 20-100nm in size, and initial-β" precipitates about 2–3 nm in diameter and nearly 8-10nm in length respectively after solution and short time aging treatment. The percentage of sub-grain boundary of the new Al-Mg-Si-Cu aluminum alloys under the forging process reach up to 72%.
2. The combination of mechanical properties of the new Al-Mg-Si-Cu aluminum alloys product in aged state show that the ductility is in a range from 15% to 18%, yield strength and tensile strength are 310MPa and 380MPa respectively, fatigue strength is range from 130MPa to 135MPa.
3. In summary, the ductility and strength of this new Al-Mg-Si-Cu aluminum alloys are 35 percent and 11 percent higher than commercial 6061 alloy. The new type of Al-Mg-Si-Cu aluminum alloys with high ductility can be used in forged wheel of commercial vehicle with one forging process.

This work was funded by Project 2016YFB0101603 supported by National Key Research and Development Program.

References

1. D. Gao, W. Nonferrous Met. 11, 174-176 (2019).
2. D. Maisonnette, M. Suery, D. Nelias, P. Chaudet, Mater. Sci. Eng. A, 528, 2718 (2011).
3. SK. Panigrahi, R. Jayaganthan, J Alloys Compd, 470, 285(2009).
4. H. Liu, Reaearch on Liquid Forging and Heat Treatment of High Strength and Toughness Aluminum Alloy Wheel: [D]. Harbin: Harbin Institute of Technology, 2015.
5. S.K. Panigrahi, R. Jayaganthan, J ALLOY COMPD, 470, 285-288 (2009).
6. S. Zhou, Study on fatigue characteristics and fracture behavior of high strength and high toughness AlMgSiCu alloy sheet: [D]. Guangxi: Guangxi University of Science and Technology, 2019.
7. D. Maisonnette, M. Suery, D. Nelias, P. Chaudet, Mater. Sci. Eng., A, **528,** 2718-2724 (2011).
8. A. Loucif, R.B. Figueiredo, T. Baudin, Mater. Sci. Eng., A, **527,** 4864-4869 (2010).
9. Y. Han, K. Ma, L. Li, H. Nagaumi. Mater. Des. **39**, 418–424 (2012).
10. J. H. Chen, C.H. Liu, Chin. J. Nonferrous Met, **21**,10(2011).
11. C. He, W. Nonferrous Met. 3, 282-283 (2018)
12. M. Murayama, K. Hono, W.F. Miao, and D.E. Laughlin, Metal. Mater. Trans. A, **32A,** 239(2001).
13. Y. Han, K. Ma, H. Nagaumi, TMS, 418–424 (2012).
14. X. Wang, S. Esmaeili, D. J. Lloyd, Metal. Mater. Trans. A, **37A,** 2006—2691 (2006).
15. G.C. Weatherly, A. Perovic, N.K. Mukhopadhyay, Metal. Mater. Trans. A, **32A,** 213(2001).
16. J. H. Chen, E. Costan, M. A. van Huis, Q. Xu, H. W. Zandbergen, SCI. **312**, 416-419 (2006).